LETTERS

Induced ncRNAs allosterically modify RNA-binding proteins *in cis* to inhibit transcription

Xiangting Wang[1,2], Shigeki Arai[5]*, Xiaoyuan Song[1]*, Donna Reichart[3], Kun Du[5], Gabriel Pascual[3,4], Paul Tempst[6], Michael G. Rosenfeld[1,4], Christopher K. Glass[3,4] & Riki Kurokawa[5]

With the recent recognition of non-coding RNAs (ncRNAs) flanking many genes[1–5], a central issue is to obtain a full understanding of their potential roles in regulated gene transcription programmes, possibly through different mechanisms[6–12]. Here we show that an RNA-binding protein, TLS (for translocated in liposarcoma), serves as a key transcriptional regulatory sensor of DNA damage signals that, on the basis of its allosteric modulation by RNA, specifically binds to and inhibits CREB-binding protein (CBP) and p300 histone acetyltransferase activities on a repressed gene target, *cyclin D1* (*CCND1*) in human cell lines. Recruitment of TLS to the *CCND1* promoter to cause gene-specific repression is directed by single-stranded, low-copy-number ncRNA transcripts tethered to the 5′ regulatory regions of *CCND1* that are induced in response to DNA damage signals. Our data suggest that signal-induced ncRNAs localized to regulatory regions of transcription units can act cooperatively as selective ligands, recruiting and modulating the activities of distinct classes of RNA-binding co-regulators in response to specific signals, providing an unexpected ncRNA/RNA-binding protein-based strategy to integrate transcriptional programmes.

Transcriptional co-regulators, including coactivators and co-repressors, are required for the regulation of programmes of gene expression in a transcription factor-specific and gene-specific manner[13,14]. Among them, the histone acetyltransferases (HATs) CBP and p300 are essential as coactivators of multiple classes of signal-dependent transcription factors[13,14]. To search for cellular factors that might regulate the HAT activity of CBP, we incubated HeLa whole-cell extracts with full-length, Flag-tagged CBP immobilized on anti-Flag IgG affinity beads (Supplementary Fig. 1a) and observed a marked inhibition of CBP HAT activity on histones (Fig. 1a). Subcellular fractionation studies indicated the presence of two classes of inhibitory activity: one that bound to CBP and was present primarily in nuclear extracts (Fig. 1a, lane 3), and the other, the INHAT complex[15], that was present in both nuclear and cytoplasmic extracts (Supplementary Fig. 2a).

The nuclear activity that inhibited CBP in pull-down HAT assays fractionated as two main peaks by gel-filtration chromatography (Fig. 1b, top, and Supplementary Fig. 1b). Pooled fractions were further purified with full-length, Flag-tagged CBP linked to anti-Flag IgG beads, on the basis of the observation that inhibitory activity was observed with full-length CBP but not with the isolated HAT domain (Supplementary Fig. 2b). A large number of proteins were recovered from the high-molecular-mass fractions and a main band of about 75 kDa in the low-molecular-mass fractions (Fig. 1c). with matrix-assisted laser desorption/ionization reflectron time-of-flight mass spectrometric (MALDI-re-TOF MS) analysis[16], this 75-kDa protein was identified in three independent purifications as TLS, an RNA-binding protein that has been suggested to function in transcription[17], RNA processing[18] and DNA repair[19–22].

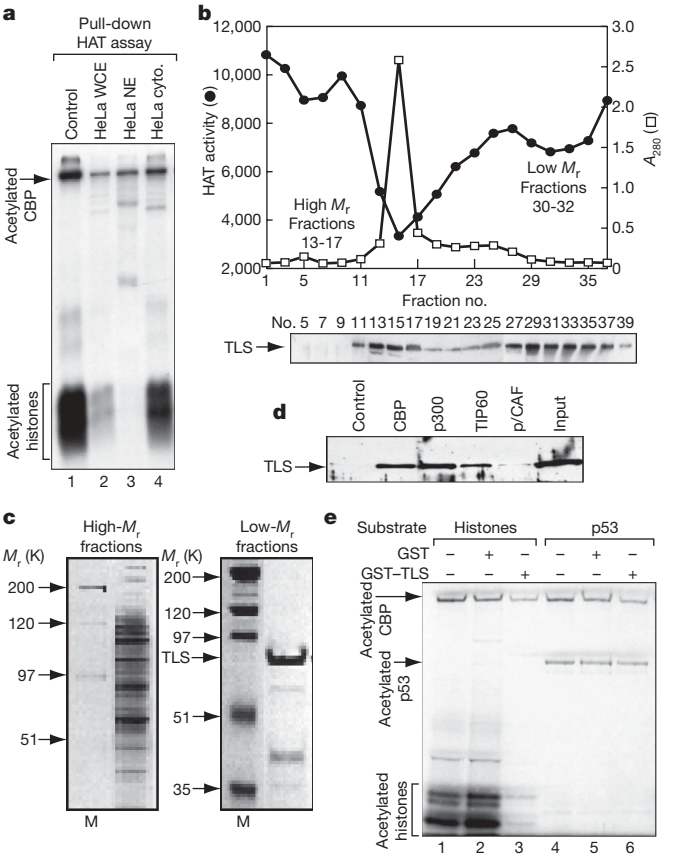

Figure 1 | TLS is a specific inhibitor of CBP and p300 HAT activity. a, CBP HAT activity measured by pull-down HAT assay. WCE, whole-cell extract; NE, nuclear extract; cyto., cytoplasmic extract. **b**, Top: inhibitory activity towards CBP HAT revealed by gel-filtration chromatography. M_r, molecular mass. Bottom: profile of TLS detected by western blotting. **c**, Representative silver-stained gels of pooled high-molecular-mass and low-molecular-mass fractions. M, molecular mass standards. **d**, TLS interacts with CBP, p300 and TIP60 but not with p/CAF. **e**, The effect of CBP HAT activity on histones or p53, determined by using GST–TLS.

[1]Howard Hughes Medical Institute, [2]Molecular Pathology Graduate Program, [3]Department of Cellular and Molecular Medicine, and [4]Department of Medicine, School of Medicine, University of California, San Diego, 9500 Gilman Drive, La Jolla, California 92093, USA. [5]Division of Gene Structure and Function, Research Center for Genomic Medicine, Saitama Medical University, 1397-1 Yamane, Hidaka-shi, Saitama-Ken, Mail code 350-1241, Japan. [6]Molecular Biology Program, Memorial Sloan-Kettering Cancer Center, New York, New York 10021, USA.
*These authors contributed equally to this work.

These findings were extended by demonstrating that recombinant TLS could bind to CBP (Fig. 1d) and strongly inhibited CBP HAT activity on core histones (Fig. 1e, lane 3). Glutathione *S*-transferase (GST)–TLS partly inhibited the acetylation of CBP itself, but not that of p53 (Fig. 1e, lane 6), suggesting that TLS selectively inhibits the ability of the acetylated CBP to transfer acetate to specific substrates. TLS also bound to p300 and TIP60 (for Tat-interacting protein 60) with similar affinities, but not to p/CAF (for p300/CBP-associated factor) (Fig. 1d and Supplementary Fig. 2c). GST–TLS inhibited the HAT activity of p300 (Fig. 2b) but not that of TIP60 (Supplementary Fig. 2d, e). TLS was also able to inhibit the acetylation by CBP of histones in nucleosomes prepared from HeLa cell nuclei (Supplementary Fig. 2f). TLS and its two related proteins EWS (for Ewing's sarcoma) and TAFII68 (for TATA-box-binding-protein-associated factor 68) (ref. 23) all proved to be present in high-molecular-mass fractions that correlate with activity that is inhibitory of CBP HAT (Fig. 1b, bottom, and Supplementary Fig. 3a). Similarly, EWS and TAFII68 were found to bind to CBP and TIP60 but not to p/CAF (Supplementary Fig. 3b, d), and exerted inhibitory effects on HAT activities of CBP and p300 (Supplementary Fig. 3c; data not shown). TLS interacted with several regions of CBP, with the region including the p160-interaction domain[24] (residues 1892–2441) serving as the most effective interaction domain (Supplementary Fig. 4). Pull-down HAT assays showed that recombinant TLS had no effect on the HAT activity of the isolated CBP_HAT region (Supplementary Fig. 2g), suggesting that the weak interaction of TLS with the CBP HAT domain (residues 1099–1877) is not sufficient for inhibitory effects towards HAT.

We next tested whether the inhibition of CBP HAT by TLS was RNA dependent. A synthetic RNA containing the consensus sequence GGUG (referred to below as the GGUG oligonucleotide) bound to TLS; mutations of GGUG to CCUC caused impaired binding[25] (Supplementary Fig. 5a). Treatment of TLS, EWS or TAFII68 with RNase A resulted in dissociation from p300 and CBP but not from TIP60 (Fig. 2a; Supplementary Fig. 5e, lanes 3–4; Supplementary Fig. 5f; Supplementary Fig. 6). Consistently, the inhibitory activity of GST–TLS on p300 HAT was abolished when GST–TLS was pretreated with the Ca^{2+}-dependent micrococcal nuclease (MNase) but not with DNase I (Fig. 2b). After blocking of MNase activity with EGTA, addition of the GGUG oligonucleotide, but not the CCUC oligonucleotide, restored the inhibitory effect of TLS on p300 HAT activity (Fig. 2b).

Interaction studies showed that the carboxy terminus of TLS (residues 211–526; 373–526 interacted with the GGUG oligonucleotide (Supplementary Fig. 5b), whereas the amino terminus (residues 1–211) interacted with CBP (Supplementary Fig. 5c).The N terminus of TLS was found to possess a detectably stronger inhibitory activity towards CBP HAT than did the full-length TLS (Supplementary Fig. 5d), and its interaction with CBP was not disrupted by treatment with RNase A (Supplementary Fig. 5e, lanes 1 and 2). Furthermore, the N terminus of TLS was capable of interacting with the C terminus of TLS (residues 373–526) in a manner that was inhibited by GGUG oligonucleotide in a dose-dependent manner (Fig. 2c), whereas the GGUG oligonucleotide enhanced the binding of TLS to p300 and CBP (Fig. 2d; data not shown). Partial proteolysis assays revealed that the GGUG oligonucleotide enhanced the cleavage of TLS (Supplementary Fig. 5g). Taken together, our findings suggest that an RNA-dependent allosteric modification of TLS relieves the inhibitory function of the C terminus of TLS, allowing the N terminus of TLS to bind to CBP and p300 and to regulate the HAT activity allosterically.

CCND1, a cell cycle regulator repressed by DNA damage signals[26], is an endogenous CREB target gene[27] and is induced in RAW264.7 cells by forskolin (Fig. 3a). Specific murine *TLS* short interfering RNA (siRNA; in this case referred to as siTLS) caused a marked increase in both basal and forskolin-stimulated *CCND1* mRNA levels in these cells (Fig. 3a and Supplementary Fig. 7a). Overexpression of human *TLS* could overcome the effect of siTLS (Supplementary Fig. 7c). Knockdown of p300 and CBP with specific siRNAs significantly decreased the acetylation of histone H3 on Lys 9 and Lys 14 (AcH3-K9K14) on the *CCND1* promoter detected by chromatin immunoprecipitation (ChIP) and *CCND1* mRNA levels (Fig. 3b, c, and

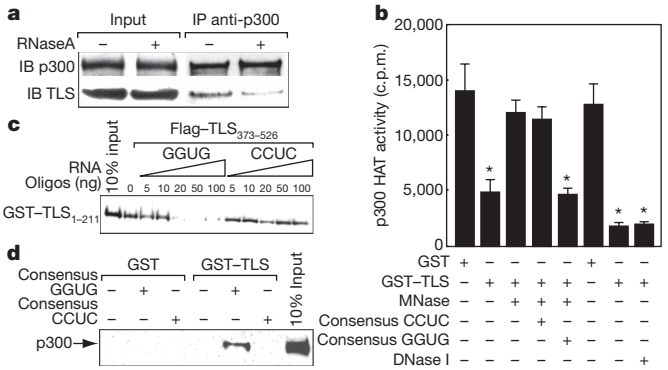

Figure 2 | Consensus GGUG-containing RNA oligonucleotide promotes the inhibitory effect of TLS on CBP and p300 HAT activities. **a**, Co-immunoprecipitation (IP) of p300 and TLS from HeLa cells treated with RNase A. **b**, p300 HAT activity was measured with micrococcal nuclease-(MNase) or DNase I-pretreated GST–TLS in the presence of GGUG or CCUC oligonucleotide. Asterisk, $P < 0.02$ compared with GST; $n = 3$. Error bars indicate s.e.m. **c**, **d**, Interaction between TLS N terminus (residues 1–211) and C terminus (residues 373–526) (**c**) or GST–TLS:p300 (**d**) in the presence of GGUG or CCUC oligonucleotide. GST and GST–TLS were pretreated with RNase A.

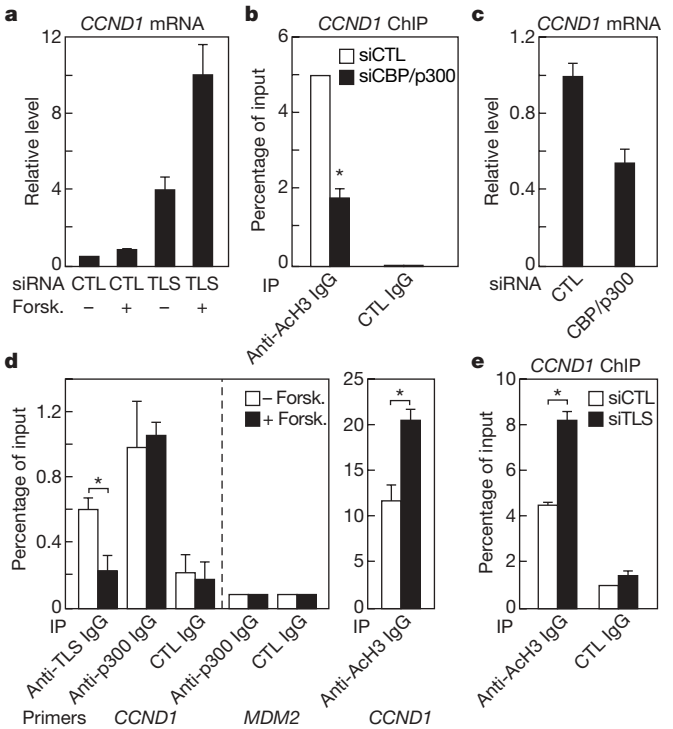

Figure 3 | TLS negatively regulates the CBP and p300 HAT-regulated *CCND1* gene. **a**, *CCND1* gene expression from RAW264.7 cells treated with forskolin (Forsk.) and *TLS* siRNA. CTL, control. **b**, **c**, Chromatin IP (ChIP) of histone acetylation (AcH3-K9K14) on the *CCND1* promoter (**b**) and *CCND1* gene expression (**c**) in the presence of control or *CBP* and *p300* siRNAs (siCBP/p300). Asterisk, $P < 0.01$; $n = 3$. **d**, ChIP with indicated immunoglobulin G (IgG) on the *CCND1* promoter on treatment with forskolin. *MDM2*, control. Asterisk, $P < 0.01$; $n = 3$. **e**, ChIP of AcH3-K9K14 on the *CCND1* promoter in the presence of control or TLS siRNA. Asterisk, $P < 0.01$; $n = 3$. Error bars indicate s.e.m.

Supplementary Fig. 7a), indicating required functions of these coactivators on this gene. Wild-type CBP, but not a HAT-mutant CBP[28], upregulated *CCND1* promoter activity (Supplementary Fig. 7b), suggesting that *CCND1* expression is dependent on the HAT function of CBP.

When RAW264.7 cells were cultured with carrier (without forskolin) in serum-starved medium, both p300 and TLS were bound to the *CCND1* promoter at the CRE site (Fig. 3d). Treatment with forskolin caused TLS to be dismissed from the *CCND1* promoter (Fig. 3d), despite a slight increase in total cellular levels of TLS (Supplementary Fig. 8a). In contrast, p300 remained bound (Fig. 3d). ChIP analysis revealed hyperacetylation of histone (AcH3-K9K14) on the *CCND1* promoter after treatment with forskolin (Fig. 3d) or knockdown of TLS (Fig. 3e). Taken together, our data suggest that TLS acts as a repressor of *CCND1*. However, we did not observe binding of TLS on all CREB targets (Supplementary Fig. 8b), suggesting that the negative regulation of CREB target genes by TLS is gene-specific.

In searching for endogenous regulatory RNAs, we took advantage of the fact that the expression of *CCND1* is downregulated in response to DNA damage signals such as those arising from ionizing radiation[29], correlated with decreased histone acetylation (Supplementary Fig. 9a, b). We considered previously unrecognized local transcripts, generated upstream of the *CCND1* promoter, as possible candidates. As shown in Fig. 4a, first-strand synthesis was performed with random primers, followed by real-time PCR with a series of validated specific primer pairs that showed similar amplification efficiencies on genomic DNA templates, spanning from −2008 to −162 base pairs upstream of the established *CCND1* transcription start site. These experiments revealed the presence of multiple previously unrecognized, ionizing-radiation-enhanced ncRNAs (A, B, D and E) transcribed from multiple 5′ regulatory regions of *CCND1* (ncRNA$_{CCND1}$; Fig. 4a). TLS interacted with these ncRNA$_{CCND1}$s as detected by RNA immunoprecipitation assays (Fig. 4b; data not shown), and a ChIP assay revealed that TLS was recruited to these ncRNA$_{CCND1}$-'expressing' regions in an ionizing-radiation-induced manner (Fig. 4c). In contrast, TLS showed very weak interaction with ncRNA$_{CCND1}$-'non-expressing' regions C and F (Fig. 4c). The level of TLS protein was never upregulated by ionizing irradiation, being either unchanged or, in some experiments, actually downregulated (Supplementary Fig. 9c).

Subcellular and chromatin fractionation studies revealed that ncRNA$_{CCND1}$ was mainly bound to chromatin (Fig. 4d). Real-time PCR analyses using several RNA species for which copy numbers have been well established as standards revealed that ncRNA$_{CCND1}$ was present at a low copy number (for example, region D at about two copies per cell under basal conditions and about four copies per cell after treatment with ionizing radiation; Fig. 4e). To test whether ncRNA$_{CCND1}$ might be present, in part, as an RNA–DNA hybrid, we evaluated the effects of treatment with RNase H and found that this treatment partly diminished ncRNA$_{CCND1}$ (Fig. 4f). A portion of ncRNAs was also diminished by RNase T1, which digests single-stranded RNA. The combination of RNase H and RNase T1 caused a complete loss of ncRNAs (Fig. 4f). This suggests that a portion of the ncRNA exists, at least transiently, as single-stranded RNA, in addition to a portion present as an RNA–DNA hybrid. TLS did not bind to the corresponding DNA sequence, nor did it bind to an RNA–DNA hybrid of the tested sequences (Fig. 4g; data not shown). ChIP for TLS on the *CCND1* promoter was performed after digestion with RNase H or RNase T1, or both. As shown in Fig. 4h, RNase T1 blocked TLS recruitment, whereas treatment with RNase H had no inhibitory effect. These data argue against RNA–DNA hybrids serving as the landing pads for TLS. Our data also revealed the presence of bidirectional ncRNA transcripts, further induced by ionizing radiation (Supplementary Fig. 10); in contrast, the adjacent 5′ untranslated region (UTR) of *CCND1* mRNA showed a decreased level in response to ionizing radiation (Supplementary Fig. 10).

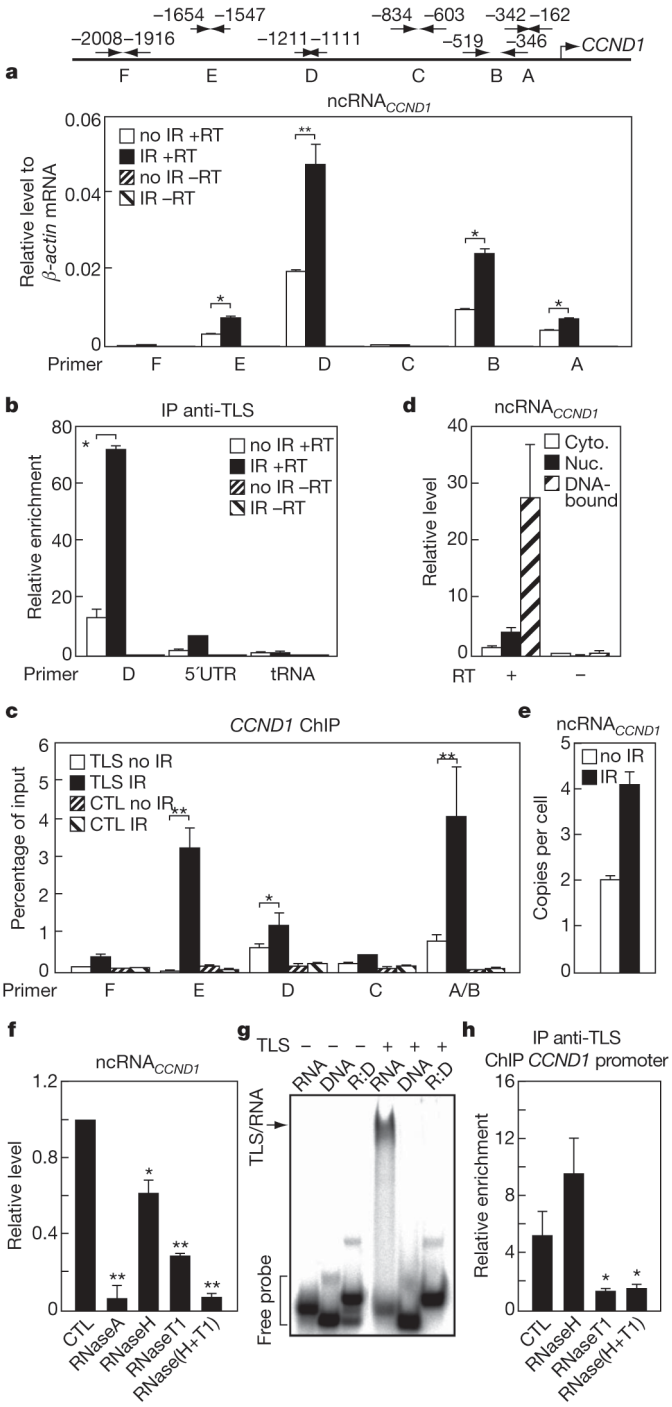

Figure 4 | ncRNA$_{CCND1}$s are predominantly single-stranded, DNA-bound species that bind to TLS. **a**, Top: diagram of ncRNA$_{CCND1}$ detection primers. Bottom: expression levels of ncRNA$_{CCND1}$s. IR, ionizing radiation; RT, reverse transcriptase. Asterisk, $P < 0.01$; two asterisks, $P < 0.002$; $n = 6$. **b**, Immunoprecipitation (IP) of TLS and detection of associated RNA by reverse transcription and real-time PCR. D, ncRNA$_{CCND1}$_D; 5′UTR, 5′ UTR of *CCND1*; transfer(t) RNA, tRNA14TyrATA. Asterisk, $P < 0.01$; $n = 3$. **c**, ChIP of TLS on the ncRNA$_{CCND1}$-'expressing' (E, D and AB) and ncRNA$_{CCND1}$-'non-expressing' regions (F and C). Asterisk, $P < 0.05$; two asterisks, $P < 0.01$; $n = 3$. CTL, control. **d**, Subcellular analysis of ncRNA$_{CCND1}$_D. **e**, Copy number of ncRNA$_{CCND1}$_D. **f**, Expression levels of ncRNA$_{CCND1}$_D on treatment with indicated RNases. Asterisk, $P < 0.05$; two asterisks, $P < 0.001$ compared with control, $n = 3$. **g**, Gel-shift analysis of TLS interactions with RNA, complementary DNA or RNA:DNA hybrid (R:D). RNA, −454s derived from ncRNA$_{CCND1}$_B. **h**, ChIP of TLS on the *CCND1* promoter on treatment with the indicated RNases. Asterisk, $P < 0.01$ compared with control; $n = 3$. Error bars indicate s.e.m.

Northern blotting analysis, with non-overlapped probes (about 200 nucleotides each) targeting the 5′ regulatory regions of *CCND1*, showed species of about 330 and about 200 nucleotides, and larger transcripts (Supplementary Fig. 11). The observations of clear variability in the lengths of these RNAs, and the fact that the bands were always multiple or diffuse, suggest diverse RNA polymerase II entry sites, or/and imprecise processing. ncRNA$_{CCND1}$ proved to be regulated by RNA polymerase II and polyadenylated, but not capped (Supplementary Fig. 12).

To investigate the potential function of ncRNA$_{CCND1}$, we identified specific siRNAs to the ncRNA$_{CCND1}$-'expressing' regions A (siA), D (siD) and E (siE); the ncRNA$_{CCND1}$-'non-expressing' regions C (siC) and F (siF); and the antisense 5′ UTR of *CCND1* (si5′UTR). SiA specifically knocked down ncRNA$_{CCND1}$ in region A without affecting that in region D; conversely, siD knocked down ncRNA$_{CCND1}$ in region D but not in region A (Supplementary Fig. 13), suggesting that multiple ncRNA transcripts were present, either as separate transcripts or as a result of rapid processing. Both strands of ncRNA$_{CCND1}$ were targeted by siA or siD (Supplementary Fig. 13). SiA, siD and siE (Fig. 5a, left), but not siC, siF or si5′UTR (Supplementary Fig. 15a), significantly enhanced the levels of endogenous *CCND1* mRNA. In contrast, the expression of *CCNE1* mRNA was not affected by either siA or siD (Fig. 5a, right). Cotransfection with siA, siD and siE (siADE) showed similar effects on the *CCND1* mRNA level compared with transfection with a single siRNA (Fig. 5a, left). As a control, the siRNA targeting the *CCND1* coding region (si*CCND1*) specifically blocked *CCND1* expression (Fig. 5a, left). These results argue against a *trans*-acting role for ncRNA$_{CCND1}$. SiD also enhanced the activity of *CCND1* promoter-driven reporter containing the ncRNA$_{CCND1}$-'expressing' region (Supplementary Fig. 14). In agreement with their putative local biological roles, siA or siD (Fig. 5b), but not siC or siF (Supplementary Fig. 15b), caused a decrease in TLS recruitment to the *CCND1* promoter at region A on treatment with ionizing radiation. In contrast, recruitment of p300 was unaffected by either siA or siD (Fig. 5b). Similar data were observed in the absence of ionizing radiation (data not shown). Neither siA nor siD decreased the level of TLS protein (Supplementary Fig. 15c). These data suggest that ncRNA$_{CCND1}$s combinatorially or cooperatively cause repression of the *CCND1* transcription unit.

Real-time PCR studies revealed the existence of ncRNA$_{CCND1}$s (D and A, but not C) in both high-molecular-mass and low-molecular-mass fractions (Supplementary Fig. 16a; data not shown). RNA oligonucleotides corresponding to the ncRNA$_{CCND1}$-'expressing' regions (for example −454s and −341a) were capable of binding to TLS and inhibiting the HAT function of p300 (Fig. 5c and Supplementary Fig. 16b, c). In contrast, a different series of RNA oligonucleotides evaluated, including oligonucleotides based on the *β-actin* mRNA sequence and the ncRNA$_{CCND1}$-'non-expressing' region C (−764a), were unable to bind to TLS (Supplementary Fig. 16d) or inhibit the HAT functions of p300 (Fig. 5c). Moreover, siA and siD, but not siC or siF, resulted in an increase in histone acetylation (AcH3-K9K14) on the *CCND1* promoter (Fig. 5d).

We suggest a model in which ncRNAs serve as molecular 'ligands' for a specific RNA-binding protein, namely TLS, causing an allosteric effect to release it from an inactive conformation. This in turn permits gene-specific TLS–CBP/p300 interactions resulting in the inhibition of HAT functions of CBP and p300 and the repression of transcription (Fig. 5e). It is tempting to speculate that other RNA-binding co-regulators exert functional roles on gene transcription by being analogously recruited to the transcription units through gene-specific ncRNAs.

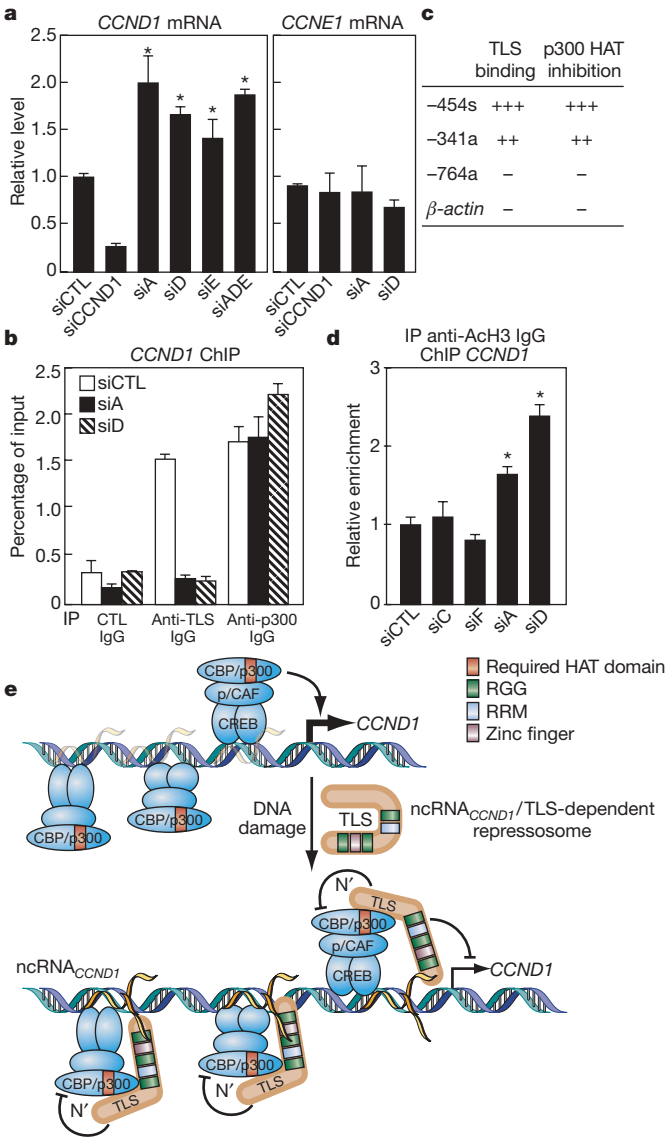

Figure 5 | ncRNA$_{CCND1}$ negatively regulates *CCND1* transcription by recruiting TLS to the *CCND1* promoter. **a**, Expression levels of *CCND1* and *CCNE1* in the presence of siRNA targeting ncRNA$_{CCND1}$_A (siA), ncRNA$_{CCND1}$_D (siD) or ncRNA$_{CCND1}$_E (siE), or by cotransfection with these siRNAs (siADE), or targeting the *CCND1*-coding region (si*CCND1*). Asterisk, $P < 0.01$ compared with control siRNA (siCTL); $n = 6$. **b**, ChIP of TLS and p300 on the *CCND1* promoter in the presence of siA or siD on treatment with ionizing radiation. **c**, RNA oligonucleotides tested for TLS binding and p300 HAT inhibition. **d**, ChIP of AcH3-K9K14 on the *CCND1* promoter in the presence of indicated siRNAs. Asterisk, $P < 0.05$; $n = 3$. Error bars in **a**, **b** and **d** indicate s.e.m. **e**, Model.

METHODS SUMMARY

RAW264.7 and HeLa cells were maintained in DMEM (Gibco) supplemented with 10% fetal calf serum (FCS; Gemini). Plasmids and siRNAs were transfected with Lipofectamine 2000 (Invitrogen) as directed. Specific antibodies were obtained from BD Biosciences (anti-TLS), Santa Cruz Biotechnology (anti-CBP and anti-p300) and Millipore (anti-acetylated histone H3).

Full Methods and any associated references are available in the online version of the paper at www.nature.com/nature.

Received 16 November 2007; accepted 9 April 2008.
Published online 28 May 2008.

1. Kapranov, P., Willingham, A. T. & Gingeras, T. R. Genome-wide transcription and the implications for genomic organization. *Nature Rev. Genet.* **8**, 413–423 (2007).
2. Bernstein, E. & Allis, C. D. RNA meets chromatin. *Genes Dev.* **19**, 1635–1655 (2005).
3. Carninci, P. *et al.* The transcriptional landscape of the mammalian genome. *Science* **309**, 1559–1563 (2005).
4. Bertone, P. *et al.* Global identification of human transcribed sequences with genome tiling arrays. *Science* **306**, 2242–2246 (2004).

5. Mattick, J. S. & Makunin, I. V. Non-coding RNA. *Hum. Mol. Genet.* **15** (Spec. Iss. 1) R17–R29 (2006).
6. Martianov, I., Ramadass, A., Serra Barros, A., Chow, N. & Akoulitchev, A. Repression of the human dihydrofolate reductase gene by a non-coding interfering transcript. *Nature* **445,** 666–670 (2007).
7. Rinn, J. L. *et al.* Functional demarcation of active and silent chromatin domains in human HOX loci by noncoding RNAs. *Cell* **129,** 1311–1323 (2007).
8. Feng, J. *et al.* The Evf-2 noncoding RNA is transcribed from the Dlx-5/6 ultraconserved region and functions as a Dlx-2 transcriptional coactivator. *Genes Dev.* **20,** 1470–1484 (2006).
9. Petruk, S. *et al.* Transcription of *bxd* noncoding RNAs promoted by Trithorax represses *Ubx* in *cis* by transcriptional interference. *Cell* **127,** 1209–1221 (2006).
10. Sanchez-Elsner, T., Gou, D., Kremmer, E. & Sauer, F. Noncoding RNAs of trithorax response elements recruit *Drosophila* Ash1 to Ultrabithorax. *Science* **311,** 1118–1123 (2006).
11. Lanz, R. B. *et al.* A steroid receptor coactivator, SRA, functions as an RNA and is present in an SRC-1 complex. *Cell* **97,** 17–27 (1999).
12. O'Neill, M. J. The influence of non-coding RNAs on allele-specific gene expression in mammals. *Hum. Mol. Genet.* **14** (Spec. Iss. 1) R113–R120 (2005).
13. Rosenfeld, M. G., Lunyak, V. V. & Glass, C. K. Sensors and signals: a coactivator/corepressor/epigenetic code for integrating signal-dependent programs of transcriptional response. *Genes Dev.* **20,** 1405–1428 (2006).
14. McKenna, N. J. & O'Malley, B. W. Combinatorial control of gene expression by nuclear receptors and coregulators. *Cell* **108,** 465–474 (2002).
15. Seo, S. B. *et al.* Regulation of histone acetylation and transcription by INHAT, a human cellular complex containing the set oncoprotein. *Cell* **104,** 119–130 (2001).
16. Sebastiaan Winkler, G. *et al.* Isolation and mass spectrometry of transcription factor complexes. *Methods* **26,** 260–269 (2002).
17. Uranishi, H. *et al.* Involvement of the pro-oncoprotein TLS (translocated in liposarcoma) in nuclear factor-κB p65-mediated transcription as a coactivator. *J. Biol. Chem.* **276,** 13395–13401 (2001).
18. Yang, L., Embree, L. J., Tsai, S. & Hickstein, D. D. Oncoprotein TLS interacts with serine-arginine proteins involved in RNA splicing. *J. Biol. Chem.* **273,** 27761–27764 (1998).
19. Hicks, G. G. *et al.* Fus deficiency in mice results in defective B-lymphocyte development and activation, high levels of chromosomal instability and perinatal death. *Nature Genet.* **24,** 175–179 (2000).
20. Kuroda, M. *et al.* Male sterility and enhanced radiation sensitivity in $TLS^{-/-}$ mice. *EMBO J.* **19,** 453–462 (2000).
21. Baechtold, H. *et al.* Human 75-kDa DNA-pairing protein is identical to the pro-oncoprotein TLS/FUS and is able to promote D-loop formation. *J. Biol. Chem.* **274,** 34337–34342 (1999).
22. Bertrand, P., Akhmedov, A. T., Delacote, F., Durrbach, A. & Lopez, B. S. Human POMp75 is identified as the pro-oncoprotein TLS/FUS: both POMp75 and POMp100 DNA homologous pairing activities are associated to cell proliferation. *Oncogene* **18,** 4515–4521 (1999).
23. Ron, D. TLS-CHOP and the role of RNA-binding proteins in oncogenic transformation. *Curr. Top. Microbiol. Immunol.* **220,** 131–142 (1997).
24. Kurokawa, R. *et al.* Differential use of CREB binding protein-coactivator complexes. *Science* **279,** 700–703 (1998).
25. Lerga, A. *et al.* Identification of an RNA binding specificity for the potential splicing factor TLS. *J. Biol. Chem.* **276,** 6807–6816 (2001).
26. Miyakawa, Y. & Matsushime, H. Rapid downregulation of cyclin D1 mRNA and protein levels by ultraviolet irradiation in murine macrophage cells. *Biochem. Biophys. Res. Commun.* **284,** 71–76 (2001).
27. Impey, S. *et al.* Defining the CREB regulon: a genome-wide analysis of transcription factor regulatory regions. *Cell* **119,** 1041–1054 (2004).
28. Murata, T. *et al.* Defect of histone acetyltransferase activity of the nuclear transcriptional coactivator CBP in Rubinstein–Taybi syndrome. *Hum. Mol. Genet.* **10,** 1071–1076 (2001).
29. Agami, R. & Bernards, R. Distinct initiation and maintenance mechanisms cooperate to induce G1 cell cycle arrest in response to DNA damage. *Cell* **102,** 55–66 (2000).

Supplementary Information is linked to the online version of the paper at www.nature.com/nature.

Acknowledgements We thank A. Gettings for help with mass spectrometric analysis; M. Hiramatsu, W. Sato and C. Nelson for technical assistance; A. Matsushita, M. Matsubara and T. Oyoshi for discussion; and J. Hightower and M. Fisher for figure and manuscript preparation. This work was supported by the Fujisawa Foundation, the Takeda Science Foundation, the Naito Foundation, Sankyo Foundation Life Science, and grants-in-aid (nos 17054036 and 18055029) from the Ministry of Education, Culture, Sports, Science, and Technology in Japan to R.K., by National Institutes of Health grants CA52599 and HL59694 to C.K.G., by National Cancer Institute Cancer Center Support grant P30 CA08748 to P.T., by NS34934, DK39949 and CA097134 to M.G.R., and by DK074868 to C.K.G. and M.G.R. M.G.R. is a Howard Hughes Medical Institute investigator.

Author Information Reprints and permissions information is available at www.nature.com/reprints. Correspondence and requests for materials should be addressed to R.K. (rkurokaw@saitama-med.ac.jp), C.K.G. (ckg@ucsd.edu) or M.G.R. (mgr@ucsd.edu).

METHODS

Materials and reagents. Antibodies were obtained from Santa Cruz Biotechnology (anti-p/CAF, anti-TAFII68 and anti-EWS), Upstate Biotechnology (anti-TIP60) and Synaptic Systems (anti-cap). siRNAs were obtained from Qiagen: siA, 5′-GGCGCCUCAGGGAUGGCUU-3′; siD, 5′-AAUUCAGUCCCAGGGCAAA-3′; siE, 5′-GACCCGGAAUAUUAGUAAU-3′; siC, 5′-GGCUAGAAGGACAAGAUGA-3′; siF, 5′-GAGUGGGCGAGCCUCUUUA-3′; si5′UTR, 5′-GGACUUUGCAACUUCAACA-3′; si*CCND1*, SI0265 4547; siCTL, 5′-AAUUCUCCGAACGUGUCAC-3′; si*TLS*, 5′-CAGAGUUA CAGUGGUUAUG-3′ and 5′-UUCUCUGGGAAUCCUAUUA-3′.

HAT assays. HeLa extracts, histones (Sigma) or mononucleosomes (from HeLa cells) and [^{14}C]acetyl-CoA were incubated with baculovirus-expressed CBP in solution HAT assays as described[30]. Pull-down HAT assays were performed by capturing baculovirus-expressed, Flag-tagged CBP on anti-Flag agarose beads (Sigma). Beads were incubated with HeLa extracts for 1 h, washed three times with HAT assay buffer, and then incubated with histones and [^{14}C]acetyl-CoA. CBP and histones were subsequently resolved by SDS–PAGE and acetylation was detected by autoradiography.

Biochemical purification and protein identification. HeLa nuclear extracts were dialysed against 0.1 M NaCl containing dialysis buffer (20 mM HEPES pH 7.9, 0.2 mM EDTA, 0.5 mM dithiothreitol (DTT)), applied to a 500-ml column of Sephacryl S-300, equilibrated, and fractionated into 43 fractions, which were analysed with HAT assay. Fractions with inhibitory activity were further incubated with baculovirus-expressed Flag-tagged CBP bound anti-Flag agarose beads and extracted with 0.3 M NaCl extraction buffer and separated by SDS–PAGE. The protein bands were analysed by matrix-assisted laser desorption/ionization reflectron time-of-flight mass spectrometry (MALDI-re-TOF MS) (UltraFlex TOF/TOF; Bruker) as described[16]. Selected peptide ions (m/z) were taken to search a 'non-redundant' human protein database (National Center for Biotechnology Information) to identify the proteins.

Gel shift assays. [^{32}P]RNA or DNA oligonucleotides (200,000 c.p.m.) were heated at 95 °C for 2 min and immediately placed on ice. RNA and its cDNA oligonucleotides were heated at 95 °C for 2 min, and annealed down to 25 °C. The probes were then incubated for 15 min at 25 °C in reaction buffer containing baculovirus-expressed TLS, 10 mM Tris-HCl pH 7.5, 5% glycerol, 10 mM EDTA, 1 mM DTT and 5 μg of yeast tRNA. The samples were then analysed on a 6% PAGE gel. The gel was dried and analysed by autoradiography. The RNA and DNA oligonucleotide sequences were as follows: GGUG oligonucleotide, 5′-UUGUAUUUUGAGCUAGUUUGGUGAC-3′; CCUC oligonucleotide, 5′-UUGUAUUUUGAGCUAGUUUCCUCAC-3′; −454s (or RNA in Fig. 4g), 5′-UCUGCCGGCUUGGAUAUGGGGUGUC-3′; −341a, 5′-CCCGGGAUUU AGGGGGUGAGGUGGA-3′; −764a, 5′-UCCAGCAGCAGCCCAAGAUGG UGGC-3′; *β-actin*, 5′-UGGCAUCGUGAUGGACUCCGGUGAC-3′; DNA, 5′-GACACCCCATATCCAAGCCGGCAGA-3′.

RNA extraction and real-time PCR. HeLa cells were lysed in RSB-100 buffer (100 mM Tris-HCl pH 7.4, 100 mM NaCl, 2.5 mM $MgCl_2$, 40 μg ml^{-1} digitonin) followed by centrifugation at 2,000*g* for 8 min. The supernatant fraction was collected as cytosolic fraction. The cell pellet was then resuspended in RSB-100 containing 0.5% Triton X-100 (RSB-100T). After centrifugation at 2,000*g* for 8 min, the supernatant was collected as nuclear fraction. The resulting cell pellet was resuspended in RSB-100T and sonicated (Fisher Sonic Dismembrator, Model 300). The soluble DNA-bound RNA fraction was collected after centrifugation at 4,000*g* for 15 min. RNA was extracted with Trizol (Invitrogen) and treated with RNase-free DNase I (DNA-free; Ambion). Reverse transcription (RT) was performed with a random hexamer or gene-specific primer. Reaction without transcriptase was performed as a no-RT control. Real-time PCR was performed with the Mx3000P (Stratagene).

RNase A, micrococcal nuclease (MNase), DNase I, RNase H and RNase T1 treatment. Whole-cell extracts of GST proteins were treated with RNase A (25 μg per 50 μl; Sigma), and incubated on ice for 20 min. GST–TLS in whole cell extracts was sequentially treated with 10 μg of micrococcal nuclease (Roche) in 100 mM sodium glycine (pH 8.6) and 10 mM $CaCl_2$ at 37 °C for 4 min, 0 °C for 1 min, and 25 °C for 20 min, and terminated by the addition of 10 mM EGTA, followed with or without incubation with RNA oligonucleotides at 100 pmol per 20 μl. GST–TLS was treated for 30 min at 37 °C with DNase I (1 μg per 50 μl) in 50 mM Tris-HCl pH 7.5, 10 mM $MgCl_2$ and 50 μg ml^{-1} BSA. For co-immunoprecipitation and RT-real time PCR, cell fractionation extracts containing the DNA-bound RNA were obtained as described before and for 30 min treated with 50 ng μl^{-1} RNase A (Sigma), RNase H (1 U per 10 μl; Invitrogen), or RNase T1 (1 U per 10 μl; Ambion) at 25 °C.

Chromatin immunoprecipitation (ChIP). Cells were crosslinked with 1% formaldehyde and stopped with glycine solution (125 mM). The cells were then sequentially washed in ice-cold buffer I (0.25% Triton X-100, 10 mM EDTA, 0.5 mM EGTA, 10 mM HEPES pH 6.5) and buffer II (200 mM NaCl, 1 mM EDTA, 0.5 mM EGTA, 10 mM HEPES pH 6.5). Cell pellets were resuspended in lysis buffer (1% SDS, 10 mM EDTA, 50 mM Tris-HCl pH 8.1, 1 × protease inhibitor cocktail) and sonicated. The soluble chromatin was then diluted in dilution buffer (1% Triton X-100, 2 mM EDTA, 150 mM NaCl, 20 mM Tris-HCl pH 8.1, 1 × protease inhibitor cocktail). Protein A/G–sepharose beads were added and incubated for 1 h at 4 °C for preclearing. Specific antibody was added to the supernatant and incubated at 4 °C. The next day, Protein A/G–sepharose beads were added and incubated for 2 h at 4 °C. Beads were harvested by centrifugation and washed sequentially in TSE I buffer (0.1% SDS, 1% Triton X-100, 2 mM EDTA, 20 mM Tris-HCl pH 8.1, 150 mM NaCl), TSE II buffer (0.1% SDS, 1% Triton X-100, 2 mM EDTA, 20 mM Tris-HCl pH 8.1, 500 mM NaCl), buffer III (0.25 M LiCl, 1% Nonidet P40, 1 mM EDTA, 10 mM Tris-HCl pH 8.1) and TE buffer. DNA fragments were eluted overnight in 1% SDS, 0.1 M $NaHCO_3$ at 65 °C and purified with a QIAquick Spin Kit (Qiagen).

RNA immunoprecipitation assay. Whole-cell extracts were obtained in NETN buffer (125 mM NaCl, 1 mM EDTA, 20 mM Tris-HCl pH 8.1, 0.5% Nonidet P40, 10% glycerol, 1 × protease inhibitor cocktail) without crosslinking, followed by sonication and preclearing as described for ChIP assay. Conjugated antibody/protein A/G–sepharose beads were pretreated with RNase inhibitor and then added for a further incubation at 4 °C overnight. Beads were then washed at least six times for 10 min each at 4 °C in NETN buffer. Bound RNA was then eluted from the beads by directly adding Trizol (Invitrogen) to the beads, followed by RNA extraction and RT-real time PCR as described previously.

30. Korzus, E. *et al.* Transcription factor-specific requirements for coactivators and their acetyltransferase functions. *Science* **279**, 703–707 (1998).